# Simulated Liquid Water and Visibility in Stratiform Boundary-Layer Clouds over Sloping Terrain

MICHAEL TJERNSTRÖM

*Department of Meteorology, Uppsala University, Uppsala, Sweden*

(Manuscript received 2 August 1991, in final form 22 February 1992)

ABSTRACT

The amount of liquid water in stratus clouds or fog is discussed from the point of view of estimating visibility variations in areas with complex terrain. The average vertical profile of liquid water from numerical simulations with a higher-order closure mesoscale model is examined, and runs with the model for moderately complex terrain are utilized to estimate the of low-level liquid water content variability and thus, indirectly, the variations in horizontal visibility along a slope.

## 1. Introduction

Accurate estimation of the amount of liquid water in stratiform boundary-layer clouds (SBLC) is a problem in meteorological applications on all scales. One key factor is the effect the amount of water has on the optical properties of the cloud. On the largest scales, it has been proposed that a global increase of low-level cloud amount of only a few percent, as a consequence of global warming, might change the atmosphere's albedo enough to offset the effect of a doubling of the $CO_2$ concentration that is causing the global warming in the first place. There is, however, relatively little hope that GCMs in the near future will be capable of reasonably accurate predictions of this type of clouds and even less that we will see good estimates of liquid water content from such models. This is due to lack of both physics in the parameterizations and of adequate vertical resolution in such models. On the other end of the scale, visibility is an important prognostic element that is strongly related to the amount of liquid water and the shape of the droplet spectrum. It is thus important to reflect on our current knowledge on how such delicate parameters as liquid water content are handled in numerical models—some of the most used tools for understanding processes in the planetary boundary layer.

The frequency of occurrence of fogs and their likely water content (translated into visibility) is one important factor to consider when planning for new airport construction. With available land becoming scarce, areas with moderately complex terrain may have to be considered. In such areas, long series of accurate observations of fog occurrence or visibility at the actual site may be scarce, and, in addition, the influence of the terrain may be difficult to access accurately. It may be insufficient to statistically correlate visibility at different locations at different terrain heights in order to assess visibility statistics at a nearby site where no observations are available. The physical process has to be considered for each observed case and an assessment has to rely on theoretical calculations and accumulated experience, for example, the measurements of the distribution of liquid water in SBLCs, the variation of visibility with relative humidity, etc. Mesoscale numerical models may also be useful to quantify the increase in liquid water in a cloud that is subjected to orographic lifting, which is the approach chosen in this paper.

The accurate simulation of liquid water in stratus and fog in such models is, however, in itself an internally important factor. In fact, it may even be questioned if some of the atmospheric boundary layer (ABL) models and in particular many mesoscale models in use today have adequate vertical resolutions for SBLC simulations, being several tenths to hundreds of meters (cf., e.g., Chen and Cotton 1983; Wai 1988; Warner et al. 1990). Such simulations have to capture a delicate balance between different processes appearing on different scales. For example, to adequately resolve the cloud-top cooling by longwave radiation processes, even when they are parameterized, probably requires a vertical resolution near the top of the cloud of the order of a few tenths of meters or less. The adequate resolution for shortwave radiative processes is probably less critical. Even if the resultant cooling and heating when including the turbulent mixing process is less sharp, that does not mean that the primary process—the differential radiative cooling and heating—can be

*Corresponding author address:* Michael Tjernström, Department of Meteorology, Uppsala University, Box 516, Uppsala, Sweden, S-751 20.

simulated with required accuracy on a coarse grid. What can happen in a model with inadequate resolution, when considering this type of cloud, is that the bulk radiative properties of the cloud may be realistic, but the model will miss the crucial partitioning of the two processes into different parts of the cloud, as well as the dynamic effect the vertical distribution of cloud water has on the distribution of turbulent production, transport, and dissipation. The amount of cooling and heating over the bulk of the cloud may be reasonably correct but will appear at the same gridpoints and thus cancel each other (see, for example, Chen and Cotton 1983) instead of cooling the cloud at the top and warming its interior. These differential radiation processes may destabilize the cloud, causing increased mixing inside the cloud, and stabilize the subcloud layer, thus decoupling the cloud and subcloud layers (Slingo et al. 1982b).

Observations of turbulence spectra inside nocturnal stratocumulus indicate that turbulent motions in this type of clouds, although labeled "stratified" in contrast to "convective," can in fact be convective (Caughey et al. 1982). This suggests that nonlocal mixing may be important and thus that local "single point" closures, where turbulent fluxes are derived from local gradients, may be questioned. Generation of turbulence close to the cloud top by differential heating and cooling also takes place primarily in the vertical wind speed component, giving rise to highly anisotropic turbulence. Many turbulence closure formulations have a limit to how much anisotropy is allowed, which is a special problem in simulations of this process (Mellor and Yamada 1982; Hassid and Galperin 1983). The situation is complicated even further by the existence of a number of different types of cloud-capped boundary layers and it is almost impossible to come up with a general set of scaling parameters applicable in all cases (Driedonks and Duynkerke 1989). Some stratus-covered ABLs are entirely driven by surface fluxes, some by radiative processes inside the cloud, and yet others by wind shear at the cloud top. A proper representation of the turbulence in SBLCs may thus, at least during certain conditions, require very different modeling tools compared to the single-point closure ensemble-average-type model used in the present study. As always, a compromise has to be struck between the need for accurate resolution and sophistication in different parameterizations on one hand and computer capacity on the other hand, in particular in 2D and 3D simulations or when a large number of simulations has to be performed for a particular practical application. The simulations presented in this paper are no exception in that respect.

One of the most used rules-of-thumb for how liquid water is distributed vertically inside a cloud is the so-called "adiabatic liquid water" profile. It relies on the assumption that the cloud is well mixed and the liquid water at any height above the cloud base is thus the difference between the vertically constant total water mixing ratio and its saturation value with respect to a temperature that varies moist adiabatically throughout the cloud. This will produce an approximately linear increase in liquid water mixing ratio with increasing height above the cloud base. One other consequence of these assumptions is that a warm cloud will contain more liquid water per kilogram of air than a cool one. The application of this theory is, however, surrounded by controversy. It is self-evident that such liquid water profiles will only exist when the underlying assumptions are valid, which is far from certain. There are a number of processes that might cause the individual cloud layer to deviate from the adiabatic values, that is, differential heating by shortwave radiation evaporating sections of the cloud partially, drizzle or cloud droplet settling causing cloud water to fall out of the cloud, and entrainment of dry air into the cloud top. Large eddy simulations (Deardorff 1980a, 1980b) show values of cloud water close to the adiabatic value for a significant portion of the cloud when entrainment is small and drizzle does not occur, as well as values well below the adiabatic for experiments with strong entrainment. Measurements during the First ISCCP (International Satellite Cloud Climatology Project) Regional Experiment (FIRE) (Albrecht et al. 1990) also show vertically integrated liquid water from a microwave radiometer close to the adiabatic values (calculated from cloud-base and cloud-top measurements performed with lidar and sodar instruments) that drops to one-half that value when drizzle occurs. Intuitively, these processes are expected to affect the upper part of the cloud most.

Many other measurements of liquid water profiles in stratiform ABL clouds also present an equally confusing picture. There are a large number of measurements in the literature of the liquid water amount increasing quasi-linearly in the vertical, in resemblance to the adiabatic liquid water profile, but at a rate less than the theoretical adiabatic values [Paltridge (1974) 30%–40%; Noonkester (1984, 1985) 50%]. Figure 1 shows one such case taken from data given by Noonkester (1984). In a number of other cases, the liquid water profile does not show any linearity with vertical distance from the cloud base at all (Tsay and Jayaweera 1984; Herman and Curry 1984; Curry and Herman 1985) and the values, as a function of distance from the cloud base, are scattered from mostly well below to occasional values above the adiabatic value (Fig. 2). This is, in particular, the case with ground based clouds, that is, fog or orographically lifted clouds. Figure 3 shows liquid water profiles from Goodman (1977) that are practically constant with height and very much lower than the corresponding adiabatic values, and Roach et al. (1976) presents measurements from a radiation fog episode where liquid water actually decreases with height. Measured cloud water near the ground in orographically lifted clouds also show values

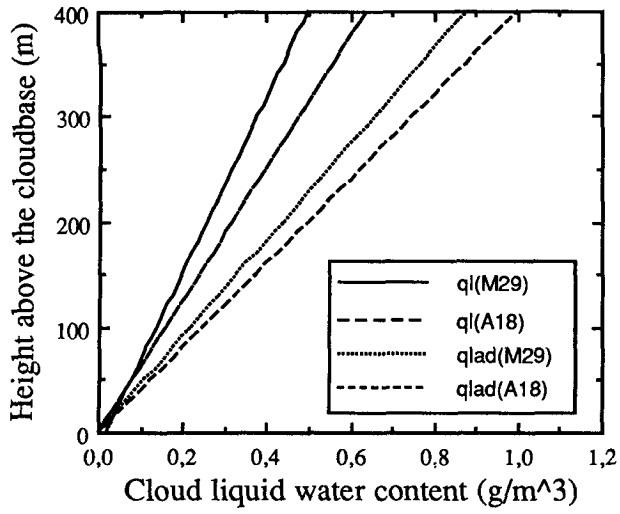


FIG. 1. Vertical variation of measured cloud water $q_l$ and corresponding adiabatic cloud water $q_{l_{ad}}$ in California stratus clouds (after Noonkester 1984).

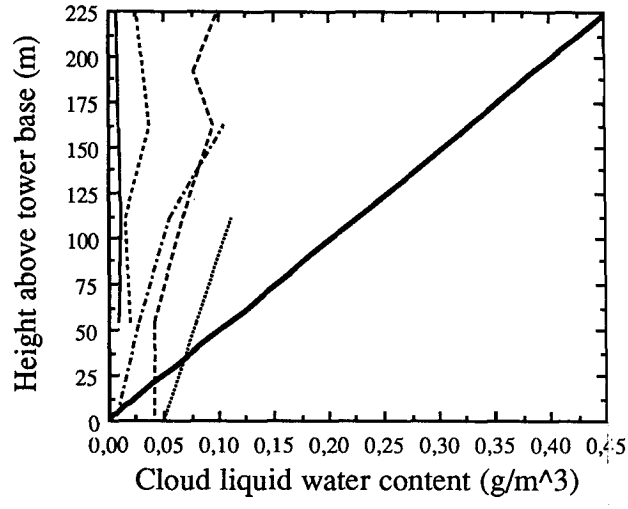


FIG. 3. Measured liquid water content in California fog and corresponding adiabatic cloud-water profile (thick solid line) (after Goodman 1977).

well above what would be expected from the simple adiabatic theory (Blyth et al. 1984; Fisher and Larsen 1984). Values of cloud water close to the ground in SBLCs above 0.3–0.4 g $m^{-3}$ are, however, rare and are often accompanied by observations of drizzle. In contrast, a number of measurements from the North Sea (Nicholls 1984; Schmetz et al. 1981, 1983) and measurements in nocturnal stratocumulus over Great Britain (Roach et al. 1982; Caughey et al. 1982; Slingo et al. 1982a; Caughey and Kitchen 1984) agree reasonably well with theoretical adiabatic values.

To summarize, the question on how the amount of liquid water normally varies vertically in SBLCs, let alone horizontally when such a cloud is lifted by orography, is far from resolved. One may expect reasonably well mixed stratus or stratocumulus clouds to feature a liquid water profile close to the adiabatic one, but one may also expect deviations to occur when processes like drizzle, entrainment, and differential radiative heating become important. In fogs, it seems reasonable to expect higher than adiabatic values close to the ground, especially in radiation fogs, simply because the temperature and humidity profiles do not exhibit any well-mixed behavior. This may change, however, as a radiation fog develops, but by then the fog might be said to have "forgotten" its origin as a radiation fog and will continue its development on its own as radiative and turbulent processes dictate. Orographically lifted SBLCs often show higher values of cloud water than expected from adiabatic theory, and the lifting of the cloud is often accompanied by a reduction in cloud-base height even relative to a reference altitude. The reduction in cloud-base height (often causing lifted clouds to reach the local ground) will produce a higher frequency of fog occurrence at higher sites compared to the frequency at nearby lower site. The higher values of liquid water will also result in poorer visibility at higher locations than at low locations for each fog episode when only episodes with fog covering both higher and lower lying areas are considered. This has to be addressed, for example, when planning for new airports.

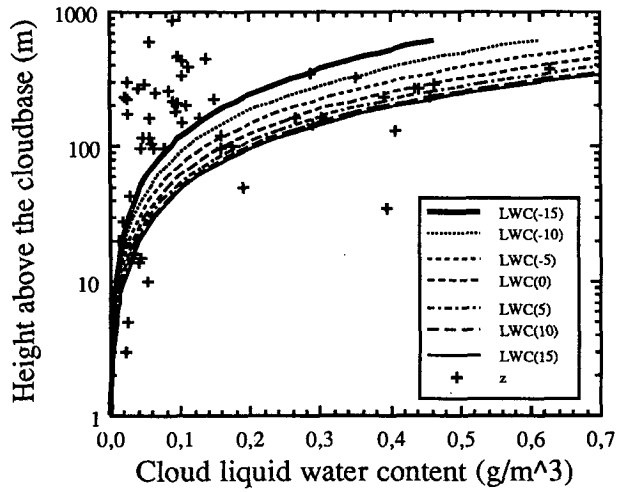


FIG. 2. Vertical variation of measured cloud-water (+) and adiabatic cloud-water profiles for different assumed values of cloud-base temperature (°C) (after Curry and Herman 1985).

## 2. Present model simulations

In an investigation on cloud formation and dissipation and the variability of the bulk properties (cloud-base and cloud-top heights) of SBLCs affected by mesoscale surface inhomogeneities, a series of simulations were performed with the Department of Meteorology, Uppsala University, Sweden, meso-γ-scale higher-order

closure model (Tjernström 1988a, 1988b). The model is hydrostatic and features a terrain-following coordinate system (Pielke and Martin 1981) in a flexible grid that is telescopic both vertically and horizontally to insure maximum resolution close to the surface and in the central area of the model domain. Turbulence is parameterized with a so-called "level 2.5" closure (Yamada and Mellor 1979; Mellor and Yamada 1974), and the model also includes parameterizations for radiation (longwave and shortwave; Chen and Cotton 1983) and for subgrid-scale condensation (Sommeria and Deardorff 1977), but not for precipitation. The cloud parameterization only yields average liquid water content in each grid box with no information on droplet size or size distribution. It is thoroughly described in Tjernström (1987a, 1987b), a shorter description is given in Tjernström (1988a), and thus a detailed description will not be given here.

In Tjernström (1988a) the effects of terrain height variations on stratus clouds or fog were studied, and these cases are investigated in more detail here with reference to liquid water profiles and the variation of cloud water along a semiconstant surface (with respect to the terrain) as the air is lifted up the slope of a 150-m-high escarpment. The slope of the escarpment is bell-shaped with a half-width of 2 km and a nominal top height of 300 m, but it is cut off at 150 m to emulate a terrain configuration typical for southern Sweden. The purpose of this study is to investigate possible effects on visibility at a proposed airport location in complex terrain with typical terrain height differences of 100–150 m under the assumption that visibility statistics are available only at upstream and/or downstream (low-elevation) locations.

### *a. Cloud-water profiles*

Since the model does not include parameterizations for drizzle, it is expected that well-developed SBLCs will feature a near-adiabatic cloud-water profile, that shallow fogs will give cloud-water values above the adiabatic, and that the cloud-water values closer to the cloud top, or for deeper clouds, will drop below the adiabatic values.

A total of 1080 upstream profiles [45 24-h simulations using output data for each hour; see Tjernström (1988a) for details on simulation procedure] were used to calculate a composite profile of cloud water as a function of distance from the cloud base. The stability for these cases were mostly ranging from stable to near neutral. To avoid bias in cloud-base height for the higher cloud bases (where the model's vertical resolution deteriorates), a procedure to define the cloud base was used. It utilizes a linear fit of temperature and dewpoint temperature between the lowest grid point with a cloud fraction above 50% and the grid point immediately below. The height where $T = T_d$ is then defined as the cloud base. The resulting composite profile for a location 20-km upstream from the top of the escarpment is shown in Fig. 4. Values of cloud water significantly above the adiabatic are found at altitudes below 70 m above the cloud base, but the variability is also largest here. Many of these cases are ground-fog episodes, and the variability thus reflects the influence of the highly variable, often nonadiabatic, temperature and humidity profiles close to the surface. The standard deviations show, however, relatively few cases with values below the expected adiabatic value. Above 70 m, the cloud water is not significantly different from the adiabatic values until an altitude of 400–500 m above the cloud base where the simulated values drops well below the adiabatic values. The variability is also reduced as altitude increases. Some of these details are clearer in Fig. 5, where the results are plotted as the ratio of the simulated to the adiabatic cloud water. The values grow as the cloud base is approached and the variability is very large; however, the actual cloud-water amounts are still small as cloud base is approached (even a large ratio times a small number can still be a small number). The high ratios close to the surface are explained by the contribution of the number of cases with stably stratified ground fogs, with large temperature gradients close to the surface, to the composite profile. These trends are basically conserved in profiles at the slope (60 m) and at the top (150 m). There is a tendency for higher ratios throughout as the terrain height increases. For low levels, this increases the already high values on average slightly, and for high levels above the cloud base, there is a tendency for the region with low ratios to approach unity.

These profiles basically show the expected features in absence of any precipitation processes, that is, higher than adiabatic cloud-water values with large variability close to the cloud base (which for many of these cases is the ground), close to adiabatic values for a large region of cloud depth, and lower than adiabatic for high levels close to the cloud top, where entrainment is expected to have an influence.

### *b. Cloud water along the slope*

Next, the variation of cloud water along the slope is examined. Only cases with fog both upstream and at the summit are considered, since the aim is to see if it is possible to deduce information on visibility, in particular poor visibility, at some height along the slope by knowing the visibility at some other (higher or lower) site in the vicinity. First, the cases from the simulations were grouped into classes according to the amount of cloud water either at the heights 3 or 7.5 m in the upstream profile. The mean variation of cloud water along the slope at these heights were then calculated for each class as the air was lifted up the slope; (constant surfaces in model coordinates are at an approximately constant height above the terrain for moderate terrain heights). The result is shown in Fig.

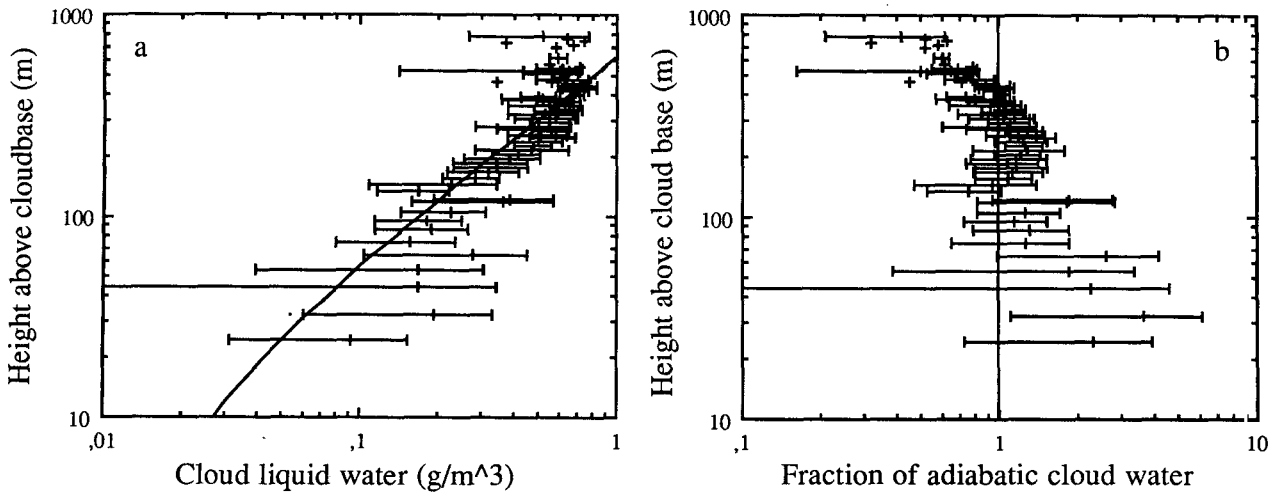


FIG. 4. (a) Composite profile of cloud water, derived from simulations, as a function of distance from cloud base from numerical simulations showing cloud water (g $m^{-3}$). (b) Ratio between simulated cloud water and adiabatic cloud water. Horizontal bars are standard deviation.

6. As somewhat of a surprise, it was found that the variation in average cloud water between the different classes was very much smaller at the top of the slope than the corresponding variation in the upstream cloud. The highest values at the top were found to be around 0.3–0.4 g $m^{-3}$, which is in accordance with measurements. The amount of cloud water in the cloud before it is lifted by orography is relatively poorly correlated to the amount of cloud water close to the surface in the lifted air. The reason for the poor correlation is seen in the difference in the shape of the frequency distribution of occurrence of cloud-water amounts close to the surface from the upstream location to the summit of the slope. At the upstream location, the maximum frequency of occurrence appears for the lowest liquid water contents. As the air is advected up the slope, the frequency distribution is altered, so that almost all the lower values disappear and the maximum frequency of occurrence is shifted to midrange values centered around 0.2 g $kg^{-1}$ (Fig. 7). This would indicate a difficulty in the use of visibility statistics for a low site to infer information about the visibility statistics at a nearby higher location. To test this, the problem was inverted and the same analysis was performed again using the cloud water amounts at the top of the escarpment as the classification criteria. The result is shown in Fig. 8. The average variation in cloud water for each class seems to be less dependent on class when the classification is performed according to the cloud water close to the ground at the top of the slope, that is, the variation between the most dry and most wet classes is roughly the same (on average) along the slope. A few cases with very little cloud water at the top and still a large amount of water in the lower area are also included. These variations are dominated by cases with dense fog capped by a strong inversion with a vertical extension of the same order of magnitude as the terrain height, thus, for the most part, confining the fog to lower areas. This illustrates the difficulty of using visibility statistics in fogs from one height to deduce information on visibility at another height. Clearly this can only be performed when selecting cases where both locations are known to be covered with fog. These results indicate that visibility statistics for poor visibility at a given site, where measurements are lacking, should be based on visibility measurements at a higher site (preferably downstream) and only for cases where both sites are covered with fog.

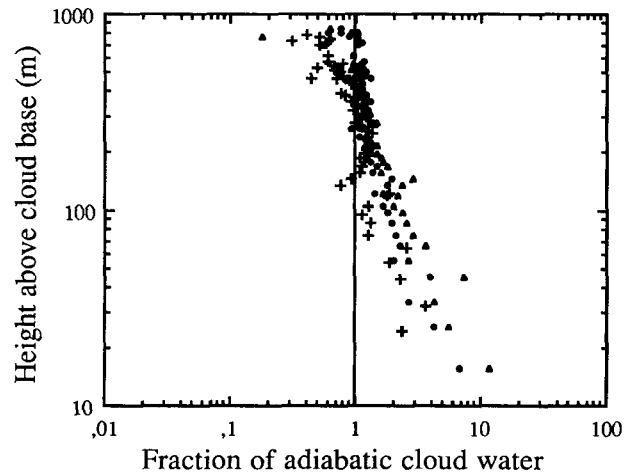


FIG. 5. As in Fig. 4b (crosses) but also including composite profiles at the slope (squares) and at the top of the terrain (triangles).

### c. *Cloud water and visibility*

To estimate the visibility quantitatively from the cloud-water data, a theoretical relationship between

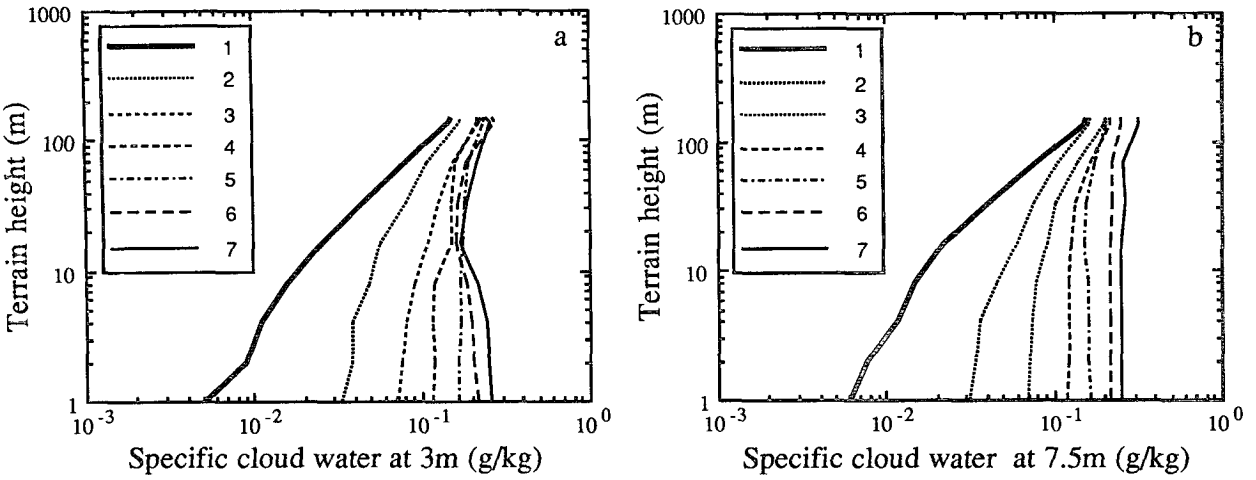


FIG. 6. Simulated cloud-water variations along the slope of a 150-m-high escarpment at (a) 3 m and (b) 7.5 m above the terrain. The cloud-water data are grouped together according to liquid water amount in the upstream undisturbed profile as 1: $q_l < 0.01$, 2: $0.01 < q_l < 0.05$, 3: $0.05 < q_l < 0.1$, 4: $0.1 < q_l < 0.15$, 5: $0.15 < q_l < 0.2$, 6: $0.2 < q_l < 0.25$, and 7: $q_l > 0.25$, where cloud-water amount is given in grams per kilogram.

visibility and cloud water must be used. Based on Beer's law, assuming a minimum contrast threshold for the human eye of 0.02, the so-called "Koshmieder" expression,

$$\text{vis} = \frac{3.912}{\sigma}; \quad \sigma \approx \sigma_s = \int_0^\infty \pi k(r) n(r) r^2 dr, \quad (1)$$

can be deduced (Jiusto 1981). Here vis is the visibility, $\sigma$ is the extinction coefficient approximated by its scattering component $\sigma_s$, $k(r)$ is the scattering area coefficient, and $n(r)$ is the number of drops in the droplet spectrum; the two latter are, in theory, functions of the droplet radius. The accuracy of this expression is mostly relative to the validity of the assumption on the minimum contrast threshold for the human eye since nothing is yet assumed about how to calculate the value for $\sigma$ other than that the extinction is dominated by scattering processes. However, $k$ is sometimes assumed to be a constant ($k = 2$) for "large drops," that is, drops with radius larger than the wavelength of visible light. A number of authors have included direct measurements of the extinction coefficient in their presentations, making it possible to calculate visibility directly from (1). One example from Noonkester (1984, 1985) is shown in Fig. 9. As detailed information on droplet spectra are difficult to obtain from case to case, this expression can be simplified further by multiplying and dividing (1) with the liquid water content $[q_l = \int_0^\infty (4/3)\pi\rho_w n(r) r^3 dr]$ and assuming it to have a constant density ($\rho_w = 1000$ kg m$^{-3}$) arriving at

$$\text{vis} = \frac{3.912\rho_w\left(\frac{4}{3}\right)\int_0^\infty n(r) r^3 dr}{2q_l \int_0^\infty n(r) r^2 dr} = \frac{2.608}{q_l} r_e, \quad (2)$$

where visibility is given in meters, droplet radius in microns, liquid water $q_l$ in grams per cubic meter, and $k \equiv 2$ is used. This equation is commonly known as the "Trabert expression" (Jiusto 1981). The drop radius $r_e$ is defined as the effective radius and is given in, for example, Curry and Herman (1985) from measurements in arctic stratus clouds. The calculated visibility as a function of altitude above the cloud base using (2) for these clouds is also given in Fig. 9. It is clear that for a cloud without contact with the ground, the visibility normally does not go below 50 m until several hundreds of meters into the cloud. With this formulation, it is also not necessary to know the details of the droplet spectrum, only its shape. For the droplet spectrum, the analytical formulation

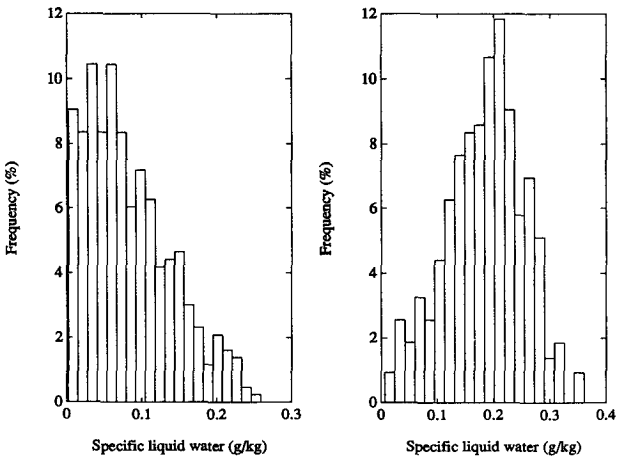


FIG. 7. Frequency distribution of occurrence of different cloud-water amount (g kg$^{-1}$) at the upstream location (left) and at the top of the escarpment (right).

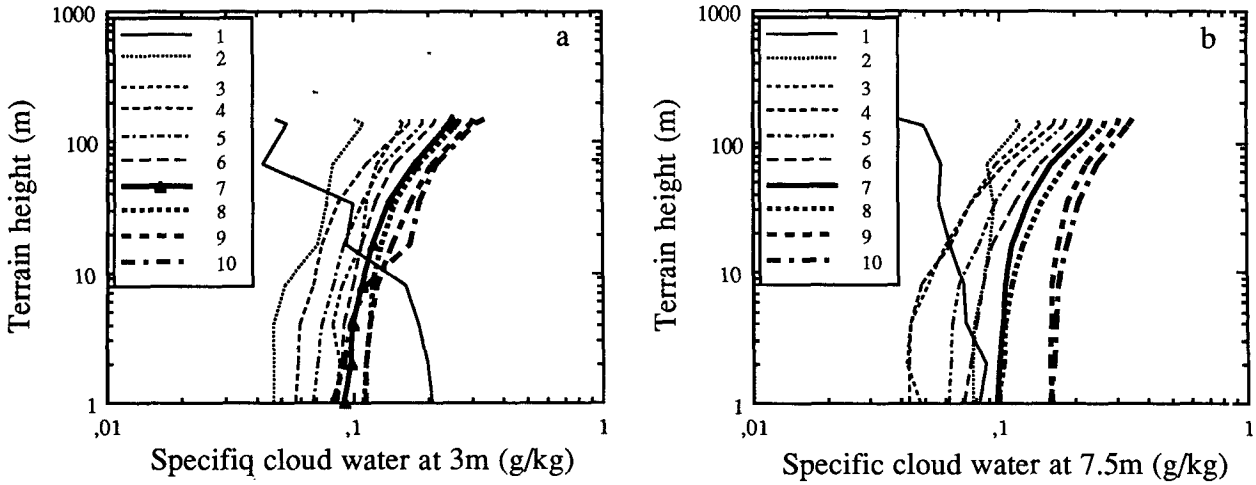


FIG. 8. As in Fig. 6 but for classes according to cloud water at the top of the slope and classes according to 1: $q_l < 0.01$, 2: $0.01 < q_l < 0.05$, 3: $0.05 < q_l < 0.1$, 4: $0.1 < q_l < 0.15$, 5: $0.15 < q_l < 0.2$, 6: $0.2 < q_l < 0.25$, 7: $0.25 < q_l < 0.3$, 8: $0.3 < q_l < 0.35$, 9: $0.35 < q_l < 0.4$, and 10: $q_l > 0.4$, where cloud-water amount is given in grams per kilogram.

$$n(r) = \frac{1}{\sigma(2\pi)^{1/2} r} e - \left[\frac{\ln^2(r/r_m)}{2\sigma^2}\right] \qquad (3)$$

from Pruppacher (1981) was chosen, where only the median droplet radius $r_m$ and the standard deviation $\sigma$ has to be chosen. After testing, it was found that the visibility was insensitive to $\sigma$ for values less than 0.2–0.3, and the value 0.1 was adopted. Figure 10 shows the relationship between the radius $r_m$ and the liquid water content for a visibility of 50 m. From this figure, comparing to Fig. 9, it is clear that episodes of very poor visibility owe their existence equally as much to the presence of small drops as to high amounts of liquid water.

The liquid water variations along the slope from the model simulations were then recalculated to visibility and the results are shown in Fig. 11, for both cases where the classification was performed according to upstream and downstream values. As the visibility becomes directly proportional to the droplet "peak" radius, this was chosen as constant, using $r_m = 10$ $\mu$m for all values of liquid water (Fisher and Larsen 1984). Several other values, ranging roughly from 1 to 20 $\mu$m appear in the literature and may be functions of such parameters as occurrence of different types and sizes of condensation nuclei that cannot be handled in this type of study. The impression from Figs. 6 and 8 reappears. When upstream cloud-water content is used, poor visibility at the lower levels results in practically no change at all, while there is a dramatic change for the cases where the visibility at the lower levels is marginal. In fact, it appears as if the visibility at the top of the slope is almost independent of visibility at the up-

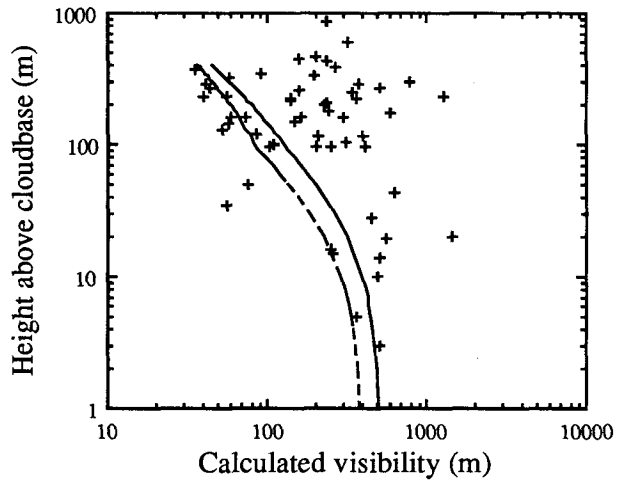


FIG. 9. Calculated values of visibility as a function of distance to the cloud base from measurements of extinction coefficient (lines, after Noonkester 1984, 1985) and measurements of effective radius (+, after Herman and Curry 1985).

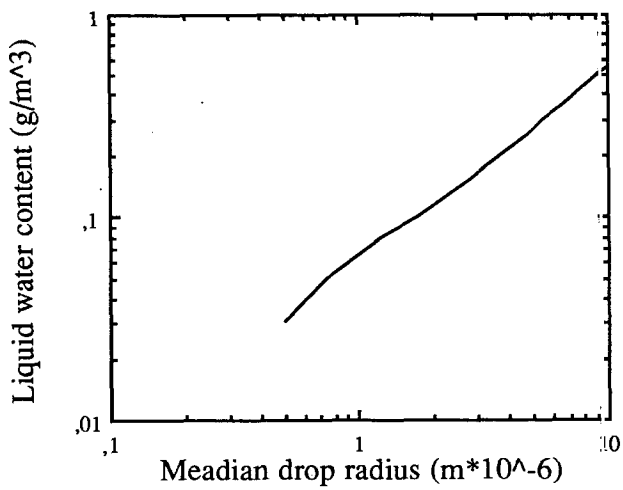


FIG. 10. Plot of the relationship between median droplet radius and cloud-water content for a calculated visibility of 50 m.

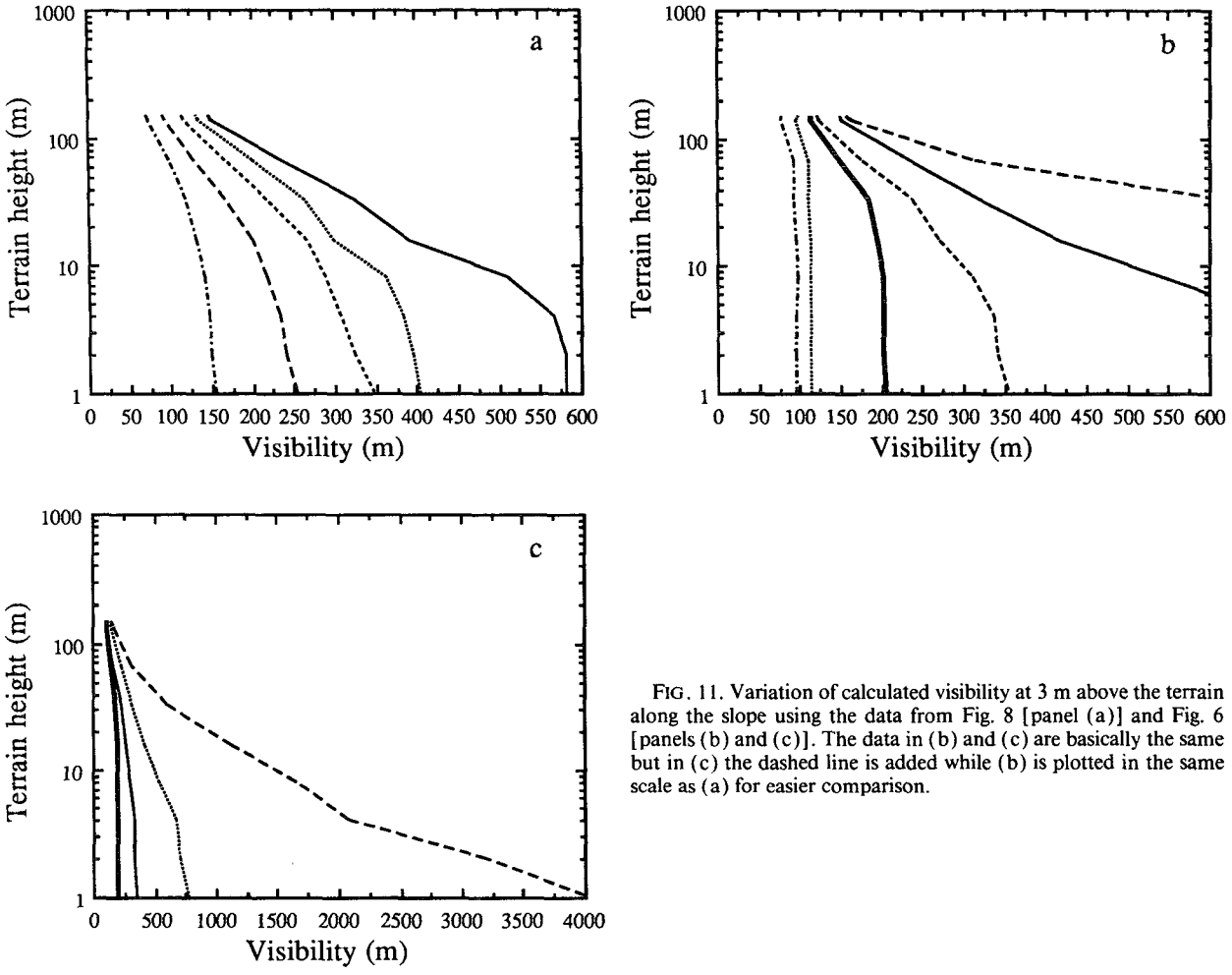


FIG. 11. Variation of calculated visibility at 3 m above the terrain along the slope using the data from Fig. 8 [panel (a)] and Fig. 6 [panels (b) and (c)]. The data in (b) and (c) are basically the same but in (c) the dashed line is added while (b) is plotted in the same scale as (a) for easier comparison.

stream low location. This will make a statistical analysis very sensitive. For the case when the downstream water content is used, the results are more continuous. Still, a variation of visibility between 70 and 150 m on average at the top corresponds to a variation between 150 and 560 m at the upstream low-lying location. It is clear that the visibility in orographically lifted SBLCs relatively rapidly becomes quite poor and that further lifting will change the visibility even less.

## 3. Discussion

The vertical and horizontal distribution of cloud water in stratiform boundary-layer clouds and its importance both as a direct output parameter from models and its consequences for the cloud dynamics has been briefly discussed. A composite vertical profile of cloud water from numerical model simulations is found to agree relatively well with theoretical expectations. On average, cloud water near the cloud base, particularly in fogs, is higher than the adiabatic cloud water; the values through a significant portion of the cloud, mostly from well-mixed situations, are close to the adiabatic values; and values at the top of the cloud drop to lower than adiabatic as entrainment becomes important. This is roughly what would be expected from a model with no parameterization of precipitation processes. The evolution and corresponding horizontal variation of cloud water in air subjected to orographic lifting has also been estimated for fog episodes. It is found that cloud water close to the ground in the lifted air is poorly correlated with cloud water in the upstream profile. The visibility variations along the slope are also estimated through a simple procedure relating cloud water and visibility using the Trabert expression with a simple lognormal formulation for the droplet spectra. The conclusion is that it will always be difficult to estimate statistics of poor visibility at a site in complex terrain solely from measurements at other locations at other altitudes. If such an attempt should be made, however, only cases with fog at both locations should be used and the measurements should be taken above and downstream from the site where the estimate is sought. The analysis for visibility from cloud-water data

is performed under the assumption that the effective droplet radius is conserved along the slope and is the same for all cases. This is probably untrue, and for a proper analysis, each case has to be evaluated separately using measured information on the visibility and preferably also the droplet spectra at least one site before making the statistical analysis.

A literature survey of droplet distributions and liquid water amounts in SBLCs gives droplets radii from a few micrometers up to 10–20 $\mu$m and liquid water contents of a few tenths of a gram per cubic meter in the lower parts of the cloud. Using the simple expressions above, it appears that fog even in heterogeneous areas should seldom result in very poor visibility (<50 m) since this would require much larger liquid water amounts than observed. Yet such poor visibility is not uncommon in reality. The answer might lie in the presence of a larger number of small drops in fog close to the surface as compared to the cloud base in ordinary clouds.

One might speculate on processes that might be responsible for this bias. There may be filtering of drops by vegetation elements, droplet settling, or washout of the larger drops in the lower layers by even larger drizzle drops from above, which would have the greatest influence on large drops and could bias droplet spectra for low-level fogs. Since many sites with moderately complex terrain, at least in Scandinavia, are covered with forests and drizzle is often observed in orographic fogs with high liquid water content, this discussion makes the assumption of a constant effective droplet radius in this study even more doubtful. Assuming a decrease in median droplet radius at the same time as the increase in liquid water content would cause an even larger visibility degradation when the air is lifted along the slope than what is calculated with the present technique.

It is clear to this author that if visibility statistics for a certain site are needed for planning purposes, special measurements have to be performed as near to this site as possible, rather than relying on statistics from existing observation stations in the vicinity but at different altitudes. Even then, numerical model calculations may have to be performed to extrapolate the data to a longer period, and it is shown here that sophisticated mesoscale modeling may be useful in this area.

*Acknowledgments.* This investigation was supported by the Swedish Meteorological and Hydrological Institute (SMHI) and the author is grateful to Mr. Bo Lindgren for useful comments and suggestions.

## REFERENCES

Albrecht, B. A., M. A. Miller, and R. M. Peters, 1990: The development of a surface-based system for observing boundary layer clouds. Reprints, *Ninth Symp. on Turbulence and Diffusion,* Roskilde, Amer. Meteor. Sci., 70–73.

Blyth, A. M., A. M. I. Chittenden, and J. Latham, 1984: An optical device for the measurement of liquid water content in clouds. *Quart. J. Roy. Meteor. Soc.*, **110,** 55–63.

Caughey, S. J., and M. Kitchen, 1984: Simultaneous measurements of turbulence and microphysical structure of nocturnal stratocumulus cloud. *Quart. J. Roy. Meteor. Soc.*, **110,** 13–34.

——, B. A. Crease, and W. T. Roach, 1982: A field study of nocturnal stratocumulus; II—turbulence structure and entrainment. *Quart. J. Roy. Meteor. Soc.*, **108,** 124–144.

Chen, C., and W. R. Cotton, 1983: A one-dimensional simulation of the stratocumulus-capped mixed layer. *Bound.-Layer Meteor.*, **25,** 289–321.

Curry, J. A., and G. F. Herman, 1985: Infrared radiative properties of summertime Arctic stratus clouds. *J. Climate Appl. Meteor.*, **24,** 525–538.

Deardorff, J. W., 1980a: Stratocumulus-capped mixed layers derived from a three-dimensional model. *Bound.-Layer Meteor.*, **18,** 495–521.

——, 1980b: Cloud top entrainment instability. *J. Atmos. Sci.*, **37,** 131–147.

Driedonks, A. G. M., and P. G. Duynkerke, 1989: Current problems in the stratocumulus-topped atmospheric boundary layer. *Bound.-Layer Meteor.*, **46,** 275–303.

Fisher, G. W., and H. R. Larsen, 1984: Hilltop measurements of cloud microphysics near Wellington. *New Zealand J. Sci.*, **27**(2), 209–218.

Goodman, J., 1977: The microstructure of California coastal fog stratus. *J. Appl. Meteor.*, **16,** 1056–1067.

Hassid, S., and B. Galperin, 1983: A turbulent energy model for geophysical flows. *Bound.-Layer Meteor.*, **26,** 397–412.

Herman, G. F., and J. A. Curry, 1984: Observational and theoretical studies of solar radiation in Arctic stratus clouds. *J. Climate Appl. Meteor.*, **23,** 5–24.

Jiusto, J. E., 1981: Fog structure. *Clouds, Their Formation, Optical Properties and Effects,* V. Hobbs and A. Deepak, Eds., Academic Press, 187–235.

Mellor, G. L., and Yamada, T., 1974: A hierarchy of turbulence closure models for planetary boundary layers. *J. Atmos. Sci.*, **31,** 1791–1806.

——, and ——, 1982: Development of a turbulence closure model for geophysical fluid problems. *Rev. Geophys. Space Phys.*, **20,** 851–875.

Nicholls, S., 1984: The dynamics of stratocumulus: Aircraft observations and comparisons with a mixed layer model. *Quart. J. Roy. Meteor. Soc.*, **110,** 783–820.

Noonkester, V. R., 1984: Droplet spectra observed in marine stratus cloud layers. *J. Atmos. Sci.*, **41,** 829–845.

——, 1985: Profiles of optical extinction coefficients calculated from droplet spectra in marine stratus cloud layers. *J. Atmos. Sci.*, **42,** 1161–1171.

Paltridge, G. W., 1974: Infrared emissivity, short-wave albedo, and the microphysics of stratiform water clouds. *J. Geophys. Res.*, **79**(27), 4053–4058.

Pielke, R. A., and Martin, C. L., 1981: The derivation of a terrain following coordinate system for use in a hydrostatic model. *J. Atmos. Sci.*, **38,** 1707–1713.

Pruppacher, H. R., 1981: The microstructure of atmospheric clouds and precipitation. *Clouds, Their Formation, Optical Properties and Effects,* V. Hobbs and A. Deepak, Eds., Academic Press.

Roach, W. T., R. Brown, S. J. Caughey, J. A. Garland, and C. J. Readings, 1976: The physics of radiation fog: I—A field study. *Quart. J. Roy. Meteor. Soc.*, **102,** 313–333.

——, ——, ——, B. Crease, and A. Slingo, 1982: A field study of nocturnal stratocumulus: I—Mean structure and budgets. *Quart. J. Roy. Meteor. Soc.*, **108,** 103–123.

Schmetz, J., E. Raschke, and H. Fimpel, 1981: Solar and thermal radiation in maritime stratocumulus clouds. *Beitr. Phys. Atmosph.*, **54**(4), 442–452.

——, A. Slingo, S. Nicholls, and E. Raschke, 1983: Case studies of radiation in the cloud-capped atmospheric boundary layer. *Proc. Royal Society discussion on 2 and 3 June 1982,* H. Charnock and R. T. Pollard, Eds., The Royal Society, London, 377–386.

Slingo, A., R. Brown, and C. L. Wrench, 1982a: A field study of nocturnal stratocumulus; III—High resolution radiative and microphysical observations. *Quart. J. Roy. Meteor. Soc.*, **108,** 145–165.

——, S. Nicholls, and J. Smetz, 1982b: Aircraft observations of marine stratocumulus during JASIN. *Quart. J. Roy. Meteor. Soc.*, **108,** 833–856.

Sommeria, G., and J. W. Deardorff, 1977: Subgrid-scale condensation in models of nonprecipitating clouds. *J. Atmos. Sci.*, **34,** 344–355.

Tjernström, M., 1987a: A study of flow over complex terrain using a three dimensional model. A preliminary model evaluation focusing on stratus and fog. *Ann. Geophys.*, **5B**(5), 469–486.

——, 1987b: A three dimensional meso-γ-scale model for studies of stratiform boundary layer clouds—A model description. Rep. No. 85, Department of Meteorology, Uppsala University, Uppsala, Sweden, 44 pp.

——, 1988a: Numerical simulations of stratiform boundary layer clouds on the meso-γ-scale. Part 1: The influence of terrain height differences. *Bound.-Layer Meteor.*, **44,** 33–72.

——, 1988b: Numerical simulations of stratiform boundary layer clouds on the meso-γ-scale. Part 2: The influence of a step change in surface roughness and surface temperature. *Bound.-Layer Meteor.*, **44,** 207–230.

Tsay, S.-C., and K. Jayaweera, 1984: Physical characteristics of Arctic stratus clouds. *J. Climate Appl. Meteor.*, **23,** 584–596.

Wai, M. M.-K., 1988: Modeling the effect of spatial varying sea surface temperature on the marine atmospheric boundary layer. *J. Appl. Meteor.*, **27,** 5–19.

Warner, T. T., M. N. Lakhtakia, J. D. Doyle, and R. A. Pearson, 1990: Marine atmospheric boundary layer circulations forced by Gulf Stream sea surface temperature gradients. *Mon. Wea. Rev.*, **118,** 309–323.

Yamada, T., and G. L. Mellor, 1979: A numerical simulation of the BOMEX-data using a turbulence closure model coupled with ensemble cloud relations. *Quart. J. Roy. Meteor. Soc.*, **105,** 915–944.